Portland Health & Air Quality

Leveraging Earth Observations and Sociodemographic Data to Assess Urban Heat Vulnerability in Portland, Maine

Spring 2025 | Massachusetts – Boston
April 4th, 2025

Authors: Mia Day (Analytical Mechanics Associates), Desirée Basail-Nicolaisen (Analytical Mechanics Associates), Conor Doremus (Analytical Mechanics Associates), Tyler Pursch (Analytical Mechanics Associates)

Abstract:
The rapid warming of the Gulf of Maine and the accelerated urbanization of Maine's coastal cities contribute to the Urban Heat Island (UHI) effect in Portland and South Portland. These cities have elevated temperatures compared to nearby rural and suburban areas due to the presence of more heat-absorbing infrastructure as well as less cooling tree canopy and vegetative cover. As a response to the intensifying UHI effect in this area, the Gulf of Maine Research Institute (GMRI) launched an Urban Heat Island Mapping project which aims to engage community members in temperature and humidity data collection for a multi-year monitoring study. GMRI partnered with NASA DEVELOP to assess the feasibility of using Earth observations to inform locations for sensor placement. We used land surface temperature (LST) data from Landsat 8 TIRS, Landsat 9 TIRS-2, and ISS ECOSTRESS data to identify UHIs. Furthermore, we created an urban heat vulnerability assessment to investigate the relationship between heat exposure and social vulnerability. We also modeled outdoor thermal comfort by calculating mean radiant temperature at the local level to further pinpoint locations for sensor placement. We found that the hottest census tracts as well as communities most vulnerable to extreme heat were located on the peninsula of Portland, suggesting a potential area for the partners to highlight when selecting where to place sensors for their UHI Mapping project. Overall, we found that it was feasible to integrate Earth observations to assess the UHI effect in Portland and South Portland.

Key Terms: Urban Heat Island effect, Landsat 8 TIRS, Landsat 9 TIRS-2, ECOSTRESS, outdoor thermal comfort, mean radiant temperature, SOLWEIG modeling, community resilience estimate

Advisors: Dr. Kenton Ross (NASA Langley Research Center), Dr. Xia Cai (NASA Langley Research Center)

Lead: Madi Arndt (MA – Boston)

1. Introduction

1.1 Project Background

The Gulf of Maine is warming faster than 95% of the world's oceans, at a rate three times the global average (Gulf of Maine Research Institute, 2023). This rapid rate of warming is due in part to changes in the Labrador Current and Gulf Stream flow patterns as these two major ocean currents meet in this region. The southward-flowing Labrador Current brings cool Arctic water to the Gulf whereas the northward-flowing Gulf Stream brings warm tropical waters. However, as a result of global climate change, the Gulf Stream is strengthening and shifting farther north, impeding the flow of the Labrador Current and leading to warmer ocean temperatures in the Gulf of Maine (Townsend et al., 2023; Gulf of Maine Research Institute, 2023). Furthermore, the Gulf's unique topography with its deep center and shallow boundaries contributes to its abnormally rapid warming. Water enters the Gulf of Maine through the Northeast Channel between the George Bank and Browns Bank, and stays enclosed within the Gulf for extended periods, further intensifying temperature increases (Gulf of Maine Research Institute, 2023).

Warming seas contribute to a wide range of environmental impacts. As water warms, it expands, leading to sea level rise, stronger storm surges, and more frequent and intense coastal flooding. Additionally, warming ocean temperatures disrupt marine ecosystems as native species migrate to cooler waters and warm-water species take over (Gulf of Maine Research Institute, 2023). On both a global and regional scale, ocean temperatures significantly influence weather and climate patterns. Typically, oceans and other bodies of water have a cooling effect on coastal land areas as they regulate air temperatures, absorb excess heat, and send a cool sea breeze over the land (Guo et al., 2022). As the Gulf of Maine has continued warming, these natural cooling effects have weakened, resulting in an increase in coastal cities' air temperatures and moisture levels, and a decrease in wind speeds (Hu, 2021). This phenomenon exacerbates the Urban Heat Island (UHI) effect in which urban temperature levels are elevated relative to temperatures in surrounding rural areas (Filho et al., 2017; Corburn, 2009). Highly developed urban areas are characterized by large heat-absorbing infrastructure, such as buildings and roadways, as well as sparse tree canopy and vegetative cover, resulting in less shade and cooling moisture. Urbanized areas also tend to exhibit both high and low temperature extremes due to a lack of vegetation to regulate the heating and cooling process (Gherri, 2023). Additionally, different types of surface material exhibit different rates of heating and cooling, and materials commonly used in urban spaces such as asphalt absorb heat readily (Kappou et al., 2002). These characteristics of urban areas are driving factors that contribute to higher year-round temperatures as well as more extreme heat days during the warm season (Filho et al., 2017).

We selected Portland and South Portland, Maine as our study area, both of which are in Cumberland County (*Figure 1*) (United States Census Bureau, 2025a; 2025b). This region is the ancestral homeland of the Aucocisco, N'dakina, and Wabanaki indigenous peoples (Native Land Digital, 2024). Located on the coast of the Gulf of Maine, the UHI effect impacts these cities due to a combination of urban development as well as a decrease in the coastal cooling capacity of the rapidly warming Gulf of Maine. Furthermore, the UHI effect is particularly intense for urban areas located in high latitude climatic zones, such as the temperature zone of Maine (Hu, 2021; Varquez & Kanda, 2018). There is stronger coupling between coastal land and ocean temperatures at high latitudes than in tropical or sub-tropical regions, further contributing to high coastal urban temperatures (Hu, 2021). Local news articles from Cumberland County highlight the severity of warming with reports of certain neighborhoods experiencing air temperature increases as high as 11.1 degrees Fahrenheit during the summer of 2024 (Overton, 2024). These extreme temperature increases are cause for community concern as they contribute to severe health impacts, especially for vulnerable groups such as elderly populations, those with pre-existing health conditions, and those without access to mitigation measures such as air conditioning (Filho et al., 2017; Overton, 2024; Valigra, 2021; Hu 2021; Maine Climate Council, 2024).

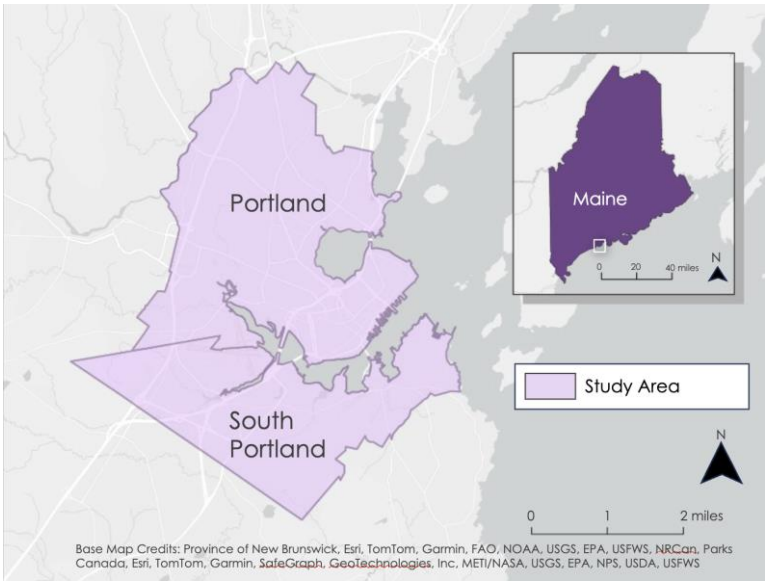

Figure 1. The cities of Portland and South Portland along the Gulf of Maine.

We partnered with the Gulf of Maine Research Institute (GMRI), a non-profit marine science center in Portland, to support their Community Science Program's Urban Heat Island Mapping project. For this project, GMRI will conduct a multi-year study into the UHI effect and its impact on the community in Portland and South Portland. GMRI aims to include community members in the data collection process through the installation of static temperature and humidity sensors at community hubs and the distribution of mobile sensors for community members to take measurements throughout the cities. GMRI will use the results of this study to identify key areas of interest within Portland and South Portland for prioritizing sensor placement. Potential areas of interest include areas found to be UHIs as well as census tracts considered the most vulnerable to heat-related health risks. As such, the results of this study inform GMRI's decision-making strategies in terms of where community members should take on-the-ground measurements to continue building knowledge surrounding the UHI effect as well as which communities are most critical to include in project outreach and engagement. GMRI's Urban Heat Mapping project will serve as a model for how to integrate remotely sensed data into community science projects monitoring the UHI effect in other communities. The findings of this study as well as GMRI's continued research will also inform Portland and South Portland's joint One Climate Future plan as well as Maine's Maine Won't Wait climate action plan, neither of which currently integrates remote sensing data into their discussion of urban heat (One Climate Future, 2020; Maine Climate Council, 2024).

1.2 Project Objectives & Scientific Basis

Our first objective was to conduct a daytime urban heat assessment using satellite data from Landsat 8 Thermal Infrared Sensor (TIRS) and Landsat 9 TIRS-2 to model the magnitude of thermal differentials indicative of UHIs. Our second objective was to conduct a nighttime urban heat assessment using ISS ECOSTRESS data to identify areas with elevated nighttime temperatures to further highlight existing UHIs. Our next objective was to investigate the relationship between extreme heat exposure and social vulnerability through the creation of a bivariate urban heat vulnerability assessment. We also aimed to model outdoor thermal comfort through calculating mean radiant temperature on a local scale for the five hottest census tracts. Our final objective was to create a tree canopy map for the cities to identify areas lacking canopy cover as these are areas with increased vulnerability to elevated urban heat temperatures. These objectives supported GMRI's Urban Heat Mapping project by identifying key locations for temperature and humidity sensors, allowing for a more intentional and targeted approach to data collection. Furthermore, the results identified communities most vulnerable to urban heat, which supports GMRI's mission to engage with

community members being impacted by extreme temperatures and build community resilience to the changing climate.

We selected a ten-year study period from 2014 to 2024 based upon our partner's interest in analyzing how observed rapid urban development shaped urban heat patterns over the past decade. We limited our analysis to the summer months of each year as the UHI effect has the greatest impact during the warm season. We defined the warm season of Portland and South Portland as June 1st through September 30th based on yearly climate reports (National Oceanic and Atmospheric Administration, 2025).

We assessed the feasibility of using NASA Earth observations (EO) and remote sensing techniques to identify UHIs and assess heat vulnerability in Portland and South Portland to support GMRI's decision-making for sensor placement. EOs are effective for identifying specific areas experiencing extreme urban heat, making them valuable for analyzing temperature distributions throughout the study area. We used data from Landsat 8 TIRS as well as Landsat 9 TIRS-2 to calculate land surface temperature (LST). These datasets enabled us to investigate the UHI effect and the broader distribution of heat across the study area. Past research demonstrates the effectiveness of utilizing TIRS data in this context (Rajasekar et al., 2009; Fu et al., 2019; Yang et al., 2020), while other studies have demonstrated its widespread use in UHI analysis (Zhou et al., 2019; Almeida., et al 2021). Furthermore, past studies used ECOSTRESS data in their analysis of nighttime temperatures (Yue et al., 2023). To inform our urban heat vulnerability assessment, we found that research indicated LST data has strong associations with heat-related human health indicators (Guo et al. 2022). Finally, we used the 3D modeling tool SOlar and Long Wave Environmental Irradiance Geometry (SOLWEIG) to model outdoor thermal comfort, a product demonstrated to be effective by Lindberg et al., 2008.

2. Methodology

2.1 Data Acquisition

2.1.1 Daytime Urban Heat Assessment

To identify areas characterized by warmer temperatures, we followed a workflow developed by a previous DEVELOP team (Miller, 2024) in Python Version 24.11.3 which extracted Landsat 8 Thermal Infrared Sensor (TIRS) and Landsat 9 TIRS-2 data from Microsoft Planetary Computer (Table 1). We used the code to compile a stack of images within the warm season (June through September) on a yearly basis for our ten-year study period. To ensure the use of clear images, we filtered out those with a high percentage of cloud cover and with high rates of no data values. This process returned between 1 and 6 images per summer.

Table 1.
Datasets acquired for the daytime urban heat assessment

Dataset	Data Product	Spatial Resolution	Time Period	Acquisition Method	Description
Landsat 8 TIRS	Collection 2 Level 2	100 m	2014 – 2021, June 01 – September 30	Planetary Computer	Long-wave infrared band to calculate LST
Landsat 9 TIRS-2	Collection 2 Level 2	100 m	2022 – 2024, June 01 – September 30	Planetary Computer	Long-wave infrared band to calculate LST
National Land Cover Database (NLCD)	Land Cover	30 m	2014 – 2024, June 01 – September 30	United States Geological Survey – Earth Explorer	Land cover data for selecting reference area

2.1.2 Nighttime Urban Heat Assessment

To conduct a nighttime urban heat assessment, we acquired geospatial datasets from the Application for Extracting and Exploring Analysis Ready Samples (AppEEARS) website. This tool allows users to subset geospatial data spatially, temporally, and by layer through area and point requests. We specified our area data via the vector polygon of Portland and South Portland and set the temporal parameters for our predetermined summer months spanning from June to September for the years 2018 - 2024. We then requested land surface temperature & emissivity (LSTE) data (ECO_L2T_LSTE.002) which included five thermal-infrared bands to calculate LST as well as available cloud mask data within the temporal parameters.

2.1.3 Urban Heat Vulnerability Assessment

To assess vulnerability to urban heat, we acquired the Community Resilience Estimate (CRE) for Heat (2022) experimental data product compiled by the United States Census Bureau. The CRE for Heat dataset provides a social vulnerability metric to describe individuals' and households' capacity to respond to extreme heat exposure. The CRE dataset takes into consideration eleven components of social vulnerability associated with heat exposure: financial hardship, single or zero caregiver's per household, low housing quality, communication barrier, no full-time employment within household, disability, no health insurance coverage, aged 65+, transportation exposure, lack of household broadband internet access, and potential lack of household air conditioning (United States Census Bureau, 2022). We downloaded the data at the census tract and national levels as a comma-separated values (CSV) file directly from the Census Bureau website.

2.1.4 Urban Heat Mitigation Model

To model outdoor thermal comfort, we used the SOlar and LongWave Environmental Irradiance Geometry (SOLWEIG) model. This model requires several spatial and meteorological data inputs to estimate and analyze the complex interaction between urban design and the thermal environment. This included a Digital Elevation Model (DEM), LiDAR Point Cloud data, building footprint data, and meteorological data (Table 2). We acquired building footprints from the Microsoft Buildings data product. Using USGS Earth Explorer, we downloaded the DEM as well as the LiDAR Point Cloud data.

Table 2.
Datasets acquired as inputs for the SOLWEIG model

Dataset	Acquisition Method	Description
USGS National Map 3D Elevation Program	United States Geological Survey – Earth Explorer	Digital Elevation Model (DEM)
USGS Maine LiDAR	United States Geological Survey – Earth Explorer	LiDAR Point Cloud data
Global Machine Learning Building Footprints	GlobalMLBuildingFootprints GitHub	Building footprint feature layer
National Renewable Energy Laboratory National Solar Radiation Database	National Solar Radiation Database (DSRDB) Viewer	Meteorological data

2.1.5 Tree Canopy Mapping

To map tree canopy cover throughout the study area, we acquired National Agriculture Imagery Program (NAIP) aerial images from the United States Department of Agriculture, downloaded from USGS Earth Explorer. We chose NAIP imagery due to its fine spatial resolution, which helped us map trees with high precision. The NAIP raster downloads included four bands (red, green, blue, and near infrared), which we utilized to classify land cover as either tree canopy or non-canopy. The data we used was from the summer of 2023 (July – September).

2.2 Data Processing

2.2.1 Daytime Urban Heat Assessment

We performed preprocessing steps on the returned images which included eliminating cloud cover, rescaling the values, and converting the data to Fahrenheit. Using the information from the QA Pixel band, we masked pixels where cloud confidence was high. We then calculated the median LST per pixel to create a composite LST image for each summer. Due to significant cloud coverage and data gap (NoData), the years 2019 and 2020 were excluded. We imported the images into ArcGIS Pro Version 3.30 and created a reference area within the town of Falmouth, a Cumberland County suburb near our study area. We used NLCD land cover datasets to select the pixels classified as vegetation within Falmouth to use as the reference area (Table 1). Selecting only those pixels classified as vegetation enabled us to contextualize the data through a comparison between urban and non-urban areas.

2.2.2 Nighttime Urban Heat Assessment

We used code from NASA's Jet Propulsion Laboratory ECOSTRESS repository in Python Version 3.13 for our data processing and analysis of nighttime urban heat temperatures. After modifying the code to perform a quality control and calibration of the dataset (Baumann, 2024a), we extracted the LST and cloud layers for applying a cloud mask (Baumann, 2024b), and created composite imagery (Baumann, 2024c; 2024d). To isolate the nighttime observations from the daytime, we filtered the data to include only observations that occurred within a pre-determined nighttime window. We defined this window as between 7:19 PM and 5:49 AM local time (11:19 PM and 9:49 AM UTC) which we found by averaging the difference between sunset times and sunrise times during the summer months.

2.2.3 Urban Heat Vulnerability Assessment

To process the data for our urban heat vulnerability assessment, we first filtered the CRE for Heat Census Tract CSV in RStudio (R Version 4.3.0) to extract census tracts within Cumberland County. We then used Microsoft Excel (Version 2502) to create a census tract number column to use as a common field for which to join the data with geospatial data. This allowed us to georeference the CRE data in ArcGIS Pro using census tract shapefiles from the United States Census Bureau to visualize the variables contained within the CSV file. Once we had the census tract shapefiles, it became clear that they did not align properly with the LST data from the daytime urban heat assessment. To rectify this, we applied a shift of 0.002 decimal degrees to the X coordinates and –0.0001 decimal degrees to the Y coordinates, whilst at a latitude of 43.6708° N (*Figure A1- A3*). With the data aligned, we visualized urban heat vulnerability by creating a bivariate vulnerability assessment. The first variable depicts heat exposure and the other describes social vulnerability. For the heat exposure variable, we used the rectified ten-year average temperature difference map.

2.2.4 Urban Heat Mitigation Model

Using QGIS Version 3.38, we converted LiDAR point cloud data to a raster using the Point Cloud Conversion Export to Raster with Triangulation tool. This created the digital surface model (DSM), a required input for the SOLWEIG model. Then, the DSM was resampled to match the spatial resolution of the DEM. To create the canopy digital surface model (CDSM) input for the SOLWEIG model, we calculated the difference between the DSM and DEM and set the pixels within building footprints to 0. Using the aggregated ten-year average temperature difference map, we identified the five hottest census tracts and clipped a copy of the DEM, DSM, and CDSM to the shape of each census tract. Then, preparing inputs for the SOLWEIG model, we reprojected, clipped, and resampled the rasters so that each input had the same shape, projection, and spatial resolution. We used the DEM, DSM, and CDSM as inputs for the Urban Multi-scale Environmental Predictor preprocessor plugin for QGIS to create other required inputs: Wall Height, Wall Aspect, and Sky View Factors.

2.2.5 Tree Canopy Mapping

To prepare the NAIP imagery for classification, we imported each of the ten raster images into ArcGIS Pro. We individually clipped each image to the study area. Working with each image individually allowed us to train the classification model more efficiently as it reduced the computing power required to run the application.

2.3 Data Analysis

2.3.1 Day-time Urban Heat Assessment

To produce our annual urban heat assessment maps, we first calculated the average temperature within the reference area for each year. To assess the UHI effect, we subtracted each year's respective reference temperature average from the entire median LST composite image for the corresponding year using the Raster Calculator in ArcGIS Pro. This method normalized each year's urban heat temperature against the broader temperature trends of that summer, allowing for a more accurate comparison between years. To create our 10-year average LST composite map, we calculated the average of these annual LST difference raster images using the raster calculator tool. Finally, we aggregated the median LST data at the census tract level using the Zonal Statistics tool in ArcGIS Pro for comparison between census tracts.

2.3.2 Nighttime Urban Heat Assessment

We created nighttime temperature composite maps on a monthly and yearly basis as well as calculated a six-year nighttime LST average using Python. The ECOSTRESS sensor was launched and installed on the International Space Station in 2018, limiting data to the six-year collection window rather than the full 10-year study period. We visualized nighttime temperatures by uploading the image outputs to QGIS version 3.40, adjusting the color ramp to appropriately reflect the temperature differential, and clipping to the study area using the Clip Raster by Mask Layer tool.

2.3.3 Urban Heat Vulnerability Assessment

To create our urban heat vulnerability assessment, we created a bivariate map to investigate the overlaps between social vulnerability factors and heat exposure. To quantify social vulnerability to heat, we used the rate of individuals who met three or more social vulnerability factors per census tract. We calculated the difference between the rate for each census tract and the national average to assess how communities within the study compared to a national baseline. We created the bivariate map in ArcGIS Pro, with one field describing social vulnerability on a scale from low to high, using a quantile distribution method to minimize the influence of any extreme values. The second field described heat exposure using the median 10-year average temperature difference between the study area and the reference area, aggregated by census tract, created as part of the daytime urban heat assessment.

2.3.4 Urban Heat Mitigation Model

To run the SOLWEIG model, we used the Urban Multi-scale Environmental Predictor plugin in QGIS. The model measures mean radiant temperature in the upward direction, downward direction, and the four cardinal directions. Mean radiant temperature captures the heat exchange between a human body and its environment. This allows the model to depict the felt temperature for areas of interest at a fine spatial resolution. Ideally, we would be able to visualize how distinct features like shadows, vegetation, and buildings influence the distribution of thermal comfort. We input the data and variables processed in section 2.2.4 and ran the model for each of the five census tracts of interest. The output raster images showed the mean radiant temperatures for the entire census tract.

2.3.5 Tree Canopy Mapping

Using the Classification Wizard tool in ArcGIS Pro, we ran an object-based supervised classification model to classify land cover into a tree canopy versus non-canopy schema. To segment the image, we set both the spectral and spatial detail to 15.0 and set the minimum segment size to 150 which aggregated the pixels without combining dissimilar landcover types. Due to running each clipped raster image individually, the spatial extent of each raster varied, which led to variation in the number of training samples we selected. For smaller raster images (up to approximately 16 km^2), we selected between 100 and 200 samples per class. As

the training samples for the tree canopy class were on average smaller in pixel size than those for non-canopy, we selected a greater number of samples representing tree canopy. For larger rasters (approximately 30 km^2), we selected upwards of 450 training samples for tree canopy and approximately 100 samples for non-canopy, ensuring that training samples were distributed throughout the entire image and included a diverse range of samples.

Upon training the model, we ran a Support Vector Machine (SVM) classifier, with no maximum number of samples per class and selected all available segment attributes for consideration. We then validated each of the outputs to ensure over 90% accuracy. We generated 100 points per class, or 200 points total, using a stratified random sample. After manually inputting whether the random point was a tree canopy or non-canopy point, we computed a confusion matrix to check the statistics on the validation.

3. Results

3.1 Analysis of Results

3.1.1 Daytime Urban Heat Assessment

When comparing the 10-year temperature difference between our study area and the reference area of Falmouth, the daytime urban heat assessment (*Figure 2*) revealed that the hottest areas are located on the peninsula of Portland and the western areas of South Portland. LST in these areas are up to 30°F hotter than the average LST from the reference area, which is consistent with the greater presence of impervious surfaces in these areas. Despite being surrounded by the ocean, the peninsula displays characteristics of a large UHI.

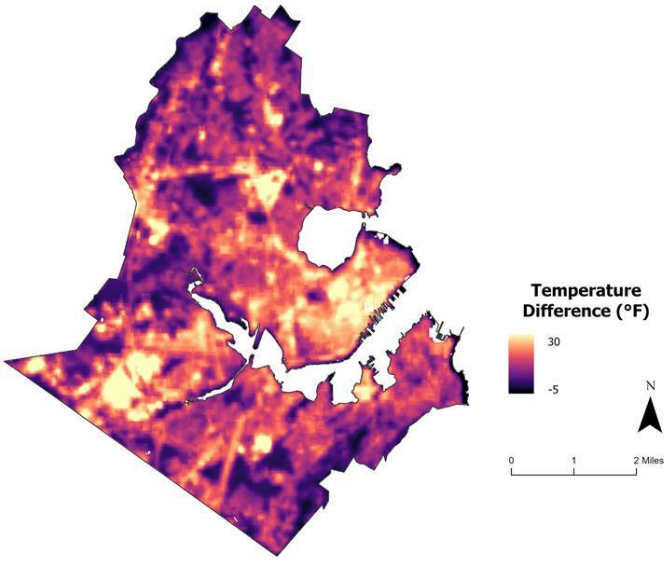

Figure 2. Daytime Urban Heat Assessment Map

3.1.2 Nighttime Urban Heat Assessment

Within the composite map that includes all nighttime summer observations between 2018 and 2024 (*Figure 3*), nighttime values produced consistently higher temperatures of 77°F maximum on the peninsula and in the middle of the city when compared with the relatively cooler temperatures further inland. While daytime UHIs have different drivers compared to nighttime UHIs in response to the presence or absence of incoming solar radiation, this heat assessment closely mirrors the daytime LST distribution. Although the temperature gradient is reduced in comparison to the daytime urban heat assessment, analysis of the nighttime results reveals a continuation and persistence of urban heat island hotspots within the study area.

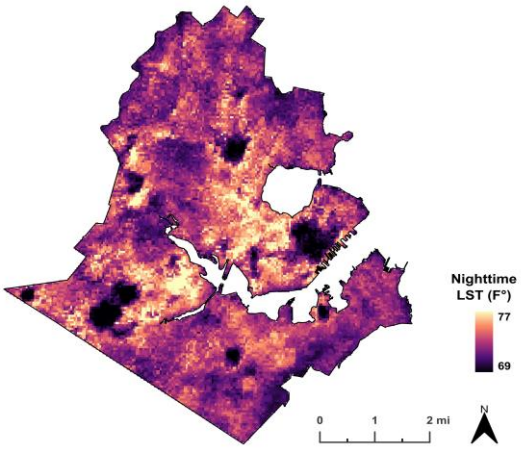

Figure 3. ECOSTRESS Nighttime Urban Heat Assessment Composite Map (2018 – 2024)

Higher temperatures of 77°F are found with Forest Avenue running along the southwest coast of the Black Cove basin on the peninsula. Notable hot spots include the intersection of Woodford Street and Forest Avenue, the cloverleaf interchange near Deering Oaks Park, and the Portland International Jetport southwest of the city center (*Figure A4*). Notable cool temperatures of 69°F are found in areas nearby or within the areas displaying higher daytime temperatures, including the Old Port area situated at the center of the peninsula, the North Deering neighborhoods near the intersection of Allen and Forest Avenue, as well as The Maine Mall on the southwestern edge of the study area (*Figure A4*).

3.1.3 Urban Heat Vulnerability Assessment

After generating a bivariate heat vulnerability map (*Figure 4*) based on the results of our daytime LST results and the Community Resilience Estimates for Heat data, we found that the census tracts with the highest median temperatures and the highest vulnerability to heat are primarily located on the peninsula of Portland. The areas with the lowest median LST and the lowest vulnerabilities tend to fall around the outskirts of the city, specifically northwest Portland and southern South Portland. We cross-referenced the results of the urban heat vulnerability assessment with a land cover map (*Figure A5*) and found that there is less urban development in the least vulnerable census tracts and more high intensity developed areas in the most vulnerable.

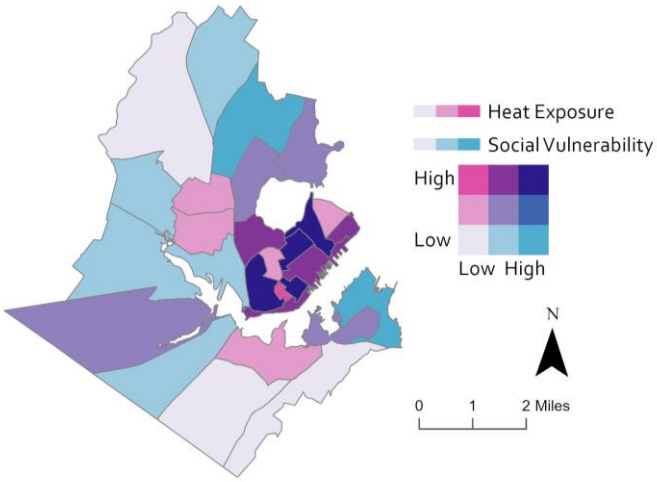

Figure 4. Urban Heat Vulnerability Assessment

3.1.4 Urban Heat Mitigation Model

The Urban Heat Mitigation Model (*Figure 5*) demonstrates the felt heat for a section of census tract 001100, one of the five hottest census tracts located on the peninsula of Portland identified using the Urban Heat Vulnerability Map. In some areas of the image, mean radiant temperatures are as high as 142°F. Building rooftops are consistently the hottest surfaces, as seen on Cumberland Ave. Some paved surfaces and roads reach similarly high temperatures, but the model shows that shade, from trees or buildings, is effective at keeping temperatures lower. The overall range of values is from 80°F to 141.8°F. We ran the model for the five hottest census tracts (*Figure A6*).

Figure 5. Subsection of Census Tract 001100 displaying Mean Radiant Temperature at 14:30 on 2 August 2020

3.1.5 Tree Canopy Mapping

The team generated a map of tree canopy cover (*Figure 6*) in order to identify locations with sparse canopy cover, as these are areas we would expect to have elevated urban heat temperatures. We cross-referenced the results of the tree canopy mapping with our daytime urban heat assessment map (*Figure 2*) as well as our urban heat vulnerability map (*Figure 4*) to investigate the relationship between these metrics. We found that notable areas with sparse vegetative cover, such as the peninsula of Portland, tend to have higher LSTs and higher vulnerability to extreme heat than areas with high canopy cover, which is consistent with our expectations given past research (Gherri, 2023; Corburn, 2009).

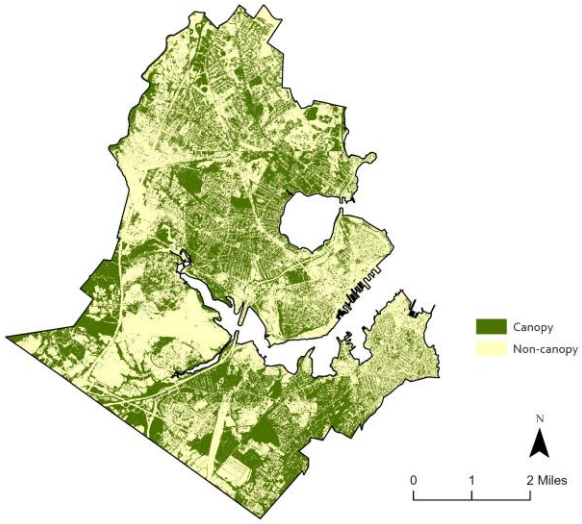

Figure 6. Tree Canopy Map (July – September 2023)

3.2 Errors & Uncertainties

One source of error stemmed from the misalignment of the LST data from other data sets during the processing phase of the daytime urban heat assessment in this study. We were unable to correct this alignment issue using the reference systems and information attached in the metadata. We resorted to shifting the data using the Shift Data Management tool in ArcGIS Pro, which allowed us to perform our analysis (*Figure A1-A3*). A manual shift is inherently less accurate than reprojection and transformation, and therefore could have introduced errors. It is worth noting as well that LST does not account for how ambient heat is experienced and therefore limited the conclusions we drew from these results.

Additionally, the results of this project were limited to the quality and availability of data. Landsat images for the daytime urban heat assessment had a coarse spatial resolution of 100 m which limited the accuracy of our LST analysis. Regarding the nighttime urban heat analysis, temperature data from AppEEARS was temporally restricted as ECOSTRESS only began collecting data in July 2018, which fell four years short of the desired 10-year study time frame for the project. There were also minor temporal limitations due in part to the irregular orbit path of the International Space Station, upon which the ECOSTRESS sensor is affixed. Because of these irregularities, some months had more nighttime observations than others which potentially skewed the average summertime composites for the years 2018 to 2024. Regarding data quality, ISS ECOSTRESS resolution is 70 m and due to the unstable nature of the satellite the images tend to be heavily pixelated. Heavily pixelated satellite images are disadvantageous when attempting to identify, analyze, and interpret data accurately.

For the urban heat vulnerability assessment, we were limited to using pre-existing vulnerability estimates such as the CRE for Heat rather than developing our own social vulnerability assessment, which prevented us from tailoring vulnerability metrics to our study area and partner interests. Furthermore, many of the social vulnerability factors were derived from estimates and proxies rather than directly measured statistics which introduced error to the CRE dataset. The CRE was available at the census tract level rather than at the block group level, which limited our ability to analyze finer nuances in vulnerability within specific communities. However, there is also a benefit to using census tract data as many of the social metrics included in the CRE would not be available at a finer scale.

Certain challenges presented themselves in the use of the SOLWEIG model as well. Given that we were unable to acquire a pre-existing CDSM for the study area, we created one by subtracting the DEM from the DSM and setting building pixels to zero. This introduced some error given that the building footprints did

not match the buildings in the DSM perfectly. The results would be more accurate if an independent CDSM was used. Additionally, SOLWEIG requires that the optional land classification input include classes that distinguish between paved areas and buildings. No such classification was readily available, nor were we able to classify the images ourselves. Including proper land classification would improve the model.

4. Conclusions

4.1 Interpretation of Results

Through our investigation of the UHI effect in Portland and South Portland, the team determined there was a consistent trend in LST distribution within the cities during the study period. Daytime LST observations revealed an increase of up to 30°F in hotspots compared to nearby vegetated areas, indicating clear urban heat islands within the cities of Portland and South Portland. We concluded that the cooling effect typically expected from the Gulf of Maine may not be an influential factor in reducing coastal land temperatures in Portland and South Portland, as the team observed no patterns indicating that areas in closer proximity to the coast exhibit cooler temperatures than those further inland. Higher humidity from the rapidly warming Gulf of Maine could explain the slow rate of cooling these areas model even as the average daytime temperature drops.

Daytime LST closely aligned with nighttime LST, and the peninsula displayed the highest temperatures across the collection of remotely sensed observations. Coastal land cover analysis data obtained from NOAA's Office for Coastal Management further confirmed that the presence of cool spots in the nighttime heat assessment could in part be attributable to the greater percentage of vegetation present in these areas helping to regulate the heating and cooling process (*Figure A5*). Our urban heat vulnerability assessment confirmed a link between urban heat exposure and social vulnerability to heat. Census tracts displaying low vulnerability and low median LST were more common in less developed areas further inland. Tracts experiencing high vulnerability to heat were in areas that also displayed the highest median temperatures, particularly on the peninsula of Portland. Community members residing in these hot spots have limited capacity to adapt to higher temperatures which suggests an area of opportunity for community outreach and engagement with those most susceptible to heat-related health risks. GMRI will be applying these findings in tandem with their outreach efforts to address this significant environmental issue impacting the region.

4.2 Feasibility & Partner Implementation

We found that it was not only feasible but also beneficial to integrate remote sensing techniques to identify the UHI effect in Portland and South Portland as satellite-derived temperature data was readily available for analysis throughout the entire study area and study period, whereas in-situ temperature measurements were unavailable for this scope. GMRI will use the end products of this project to support their Community Science Program's Urban Heat Island Mapping project to identify areas of interest for continued monitoring. The main goal of their project is to engage community members in the data collection process by installing static temperature and humidity sensors at community centers and local hubs such as schools and libraries, as well as by distributing mobile sensors to data collection participants for measurement collection along commuting routes. The urban heat vulnerability assessment will be used to help meet the partner's goals of building community resilience through outreach initiatives that engage with those most at-risk to extreme heat exposure and the associated negative health impacts. Furthermore, the partners can adapt this project's urban health vulnerability methodology to include different metrics relevant to future project interests. GMRI's Urban Heat Island Mapping project will serve as a model for how to integrate remote sensing data into future projects investigating the UHI effect in other communities in Maine and across the country. The findings of this study, as well as GMRI's future research, will also inform Portland and South Portland's joint One Climate Future plan as well as the Maine Won't Wait Climate Action Plan led by the state of Maine. The project's non-profit partner and local collaborators will both share these project results and use the end products to build climate resilience against the threats of extreme heat due to the UHI effect.

5. Acknowledgements

The Spring 2025 NASA DEVELOP Portland Heat & Air Quality team would like to thank our partner, The Gulf of Maine Research Institute, for their collaboration and assistance with this project. The team is grateful for the technical direction and feedback imparted by our science advisors, Dr. Kenton Ross and Dr. Xia Cai, and appreciates the additional support provided by Caroline Baumann and Isabel Tate. The team would also like to extend a thank you to our Node Lead, Madi Arndt, who provided our team with invaluable support and guidance to ensure this project was a success.

Any opinions, findings, and conclusions or recommendations expressed in this material are those of the author(s) and do not necessarily reflect the views of the National Aeronautics and Space Administration.

This material is based upon work supported by NASA through contract 80LARC23FA024.

6. Glossary

AppEEARS – The Application for Extracting and Exploring Analysis Ready Samples
CDSM – Canopy Digital Surface Model
CRE – Community Resilience Estimate
DEM – Digital Elevation Model
DSM – Digital Surface Model
Earth observations – Satellites and sensors that collect information about the Earth's physical, chemical, and biological systems over space and time.
ECOSTRESS – Ecosystem Spaceborne Thermal Radiometer Experiment on Space Station
Emissivity – The relative power of a surface to emit heat by radiation
Labrador Current – A current that flows south along the western boundary of the Labrador Sea located in the North Atlantic Ocean.
LiDAR – Light Detection and Ranging
LST – Land Surface Temperature
Gulf Stream – An ocean current that runs along the east coast of the United States and Canada, delivering the warm water from the Gulf of Mexico to the northern Atlantic Ocean.
GMRI – The Gulf of Maine Research Institute
ISS – International Space Station
Median – a value or quantity located at the midpoint of observed values or quantities.
Mitigation – reducing the severity or seriousness of something
NAIP – National Agriculture Imagery Program
NASA – National Aeronautics and Space Administration which is a United States government agency that is responsible for science and technology related to air and space.
NDVI – Normalized Difference Vegetation Index which quantifies vegetation by measuring the difference between near-infrared, which vegetation strongly reflects, and red light, which vegetation absorbs.
OLI – Operational Land Imager
Remote sensing – the scanning of the Earth by satellite or high-flying aircraft in order to obtain information about it.
Shapefile – simple, nontopological format for storing the geometric location and attribute information of geographic features.
SOLWEIG – SOlar and Long Wave Environmental Irradiance Geometry
Temporal – relating to time
Thermal – relating to heat energy
TIRS – Thermal Infrared Sensor
Urban Heat Island – A phenomenon that occurs when a developed area experiences higher temperatures than nearby rural areas.

7. References

Ahmad, B., Najar, M. B., & Ahmad, S. (2024). Analysis of LST, NDVI, and UHI patterns for urban climate using Landsat-9 satellite data in Delhi. *Journal of Atmospheric and Solar-Terrestrial Physics*, *265*, 106359. https://doi.org/10.1016/j.jastp.2024.106359

Almeida, C. R. D., Teodoro, A. C., & Gonçalves, A. (2021). Study of the urban heat island (UHI) using remote sensing data/techniques: A systematic review. *Environments*, 8(10), 105. https://doi.org/10.3390/environments8100105

Baumann, C. (2024a). *Applying QC Flags - ECOSTRESS Tutorial.* Applying QC Flags. https://ecostress.jpl.nasa.gov/downloads/tutorials/Applying_QC_Flags.pdf

Baumann, C. (2024b). *Batch Cloud Masking - ECOSTRESS Tutorial.* Batch Cloud Masking. https://ecostress.jpl.nasa.gov/downloads/tutorials/Batch_Cloud_Masking.pdf

Baumann, C. (2024c). *Creating a Composite Image - ECOSTRESS Tutorial.* Creating a Composite Image. https://ecostress.jpl.nasa.gov/downloads/tutorials/Creating_a_Composite_Image.pdf

Baumann, C. (2024d). *Creating Monthly Composites - ECOSTRESS Tutorial.* Creating Monthly Composites. https://ecostress.jpl.nasa.gov/downloads/tutorials/Creating_Monthly_Composites.pdf

Corburn, J. (2009). Cities, climate change and urban heat island mitigation: Localising global environmental science. *Urban Studies*, *46*(2), 413–427. https://doi.org/10.1177/0042098008099361

Filho, W., Echevarria-Icaza, L., Neht, A., Klavins, M., & Morgan, E. (2017). Coping with the impacts of urban heat islands. A literature-based study on understanding urban heat vulnerability and the need for resilience in cities in a global climate change context. *Journal of Cleaner Production,* 171, 1140–1149. https://doi.org/10.1016/j.jclepro.2017.10.086

Gherri, B. (2023). The Role of Urban Vegetation in Counteracting Overheating in Different Urban Textures. *Land*, *12*(12), 2100. https://doi.org/10.3390/land12122100

Guo, F., Zhao, J., Zhang, H., Dong, J., Zhu, P., Lau, S.S.Y. (2022). Effects of urban form on sea cooling capacity under the heatwave. *Sustainable Cities and Society*, 88, 104271. https://doi.org/10.1016/j.scs.2022.104271

Gulf of Maine Research Institute (2023, August 17). *Gulf of Maine, Explained: Causes & Impacts of Rapid Warming.* Gulf of Maine Research Institute. https://www.gmri.org/stories/gulf-of-maine-explained-causes-impacts-of-rapid-warming/

Hu, L. (2021). A global assessment of coastal marine heatwaves and their relation with coastal urban thermal changes. *Geophysical Research Letters*, 48, e2021GL093260. https://doi.org/10.1029/2021GL093260

Kannan, S., Kerwin, P., Miller, K., & Tu, E. (2024). *San José Urban Development: Quantifying Canopy Cover and Land Surface Temperature in San José to Identify Future Tree Planting Sites* [Unpublished manuscript]. NASA DEVELOP National Program, Virginia – Langley.

Kappou, S., Souliotis, M., Papaefthimiou, S., Panaras, G., Paravantis, J. A., Michalena, E., Hills, J. M., Vouros, A. P., Ntymenou, A., & Mihalakakou, G. (2022). Cool Pavements: State of the Art and New Technologies. *Sustainability*, *14*(9), 5159. https://doi.org/10.3390/su14095159

Lindberg, F., Holmer, B., & Thorsson, S. (2008). SOLWEIG 1.0 – Modelling spatial variations of 3D radiant fluxes and mean radiant temperature in complex urban settings. *International Journal of Biometeorology*, 52(7), 697–713. https://doi.org/10.1007/s00484-008-0162-7

Miller, K. (2024). Land Surface Temperature acquired from Microsoft Planetary Computer (microsoft/PlanetaryComputer 2022). [Unpublished code]. NASA DEVELOP.

Maine Climate Council. (2024). *Maine Won't Wait: A Four-Year Plan for Climate Action*. Maine. https://www.maine.gov/climateplan/sites/maine.gov.climateplan/files/2024-11/MWW_2024_Book_112124.pdf

National Oceanic and Atmospheric Administration. (2025). *Climate Information Library – National Weather Service Portland Gray Maine*. National Weather Service. https://www.weather.gov/gyx/climate_f6.html

Native Land Digital. (2024). *Native Land Map*. Native Land Digital. https://native-land.ca/

One Climate Future. (2020). One Climate Future: Charting a Course for Portland and South Portland. Portland and South Portland. https://www.oneclimatefuture.org/

Overton, P. (2024, July 10). *South Portland and Portland downtowns are Maine's hottest 'heat islands'*. Portland Press Herald. https://www.pressherald.com/2024/07/10/south-portland-and-portland-downtowns-are-maines-hottest-heat-islands

Rajasekar, U., & Weng, Q. (2009). Spatiotemporal modelling and analysis of urban heat islands by using Landsat TM and ETM+ imagery. *International Journal of Remote Sensing*, *30*(13), 3531–3548. https://doi.org/10.1080/01431160802562289

Townsend, D. W., Pettigrew, N. R., Thomas, M. A., Moore, S. (2023). Warming waters of the Gulf of Maine: The role of shelf, slope and Gulf Stream water masses. *Progress in Oceanography,* 215, 103030. https://doi.org/10.1016/j.pocean.2023.103030

United States Census Bureau. (2024). *2022 Community Resilience Estimates for Heat*. United States Census Bureau. https://www.census.gov/data/experimental-data-products/cre-heat.html

United States Census Bureau. (2022). *2022 Community Resilience Estimates for Heat: Quick Guide*. United States Census Bureau. https://www2.census.gov/programs-surveys/demo/datasets/community-resilience/2022/heat/CRE_Heat_Quickguide_2022.pdf

United States Census Bureau. (2025). *Portland city, Maine*. United States Census Bureau. https://data.census.gov/profile/Portland_city,_Maine?g=160XX00US2360545#populations-and-people

United States Census Bureau. (2025) *South Portland city, Cumberland County, Maine*. United States Census Bureau.

https://data.census.gov/profile/South_Portland_city,_Cumberland_County,_Maine?g=060XX00US2300571990

United States Department of Agriculture. National Agriculture Imagery Program (NAIP) [Dataset]. USDA. https://naip-usdaonline.hub.arcgis.com/

United States Geological Survey. Landsat 8-9 Operational Land Imager (OLI) and Thermal Infrared Sensor (TIRS) Collection 2, Level 2, Tier 1 Surface Temperature [Dataset]. USGS. https://planetarycomputer.microsoft.com/dataset/landsat-c2-l2

United States Geological Survey (2021). *20211029, USGS Original Product Resolution ME_SouthCoastal_2020_A20 19TCH360797* [Dataset]. USGS. https://portal.opentopography.org/usgsDataset?dsid=ME_SouthCoastal_1_2020

United States Geological Survey (2024). *20240617, USGS 1/3 Arc Second n44w071 20240617* [Dataset]. USGS. https://nationalmap.gov/elevation.html

Valigra, L. (2021, July 14). *Portland is a "heat island" - and it's only getting hotter.* Maine Public. https://www.mainepublic.org/environment-and-outdoors/2021-07-14/portland-is-a-heat-island-and-its-only-getting-hotter

Varquez, A.C.G. & Kanda, M. (2018). Global urban climatology: a meta-analysis of air temperature trends (1960-2009). *Climate and Atmospheric Science.* 1(32). https://doi.org/10.1038/s41612-018-0042-8

Yang, Z., Witharana, C., Hurd, J., Wang, K., Hao, R., & Tong, S. (2020). Using Landsat 8 data to compare percent impervious surface area and normalized difference vegetation index as indicators of urban heat island effects in Connecticut, USA. *Environmental Earth Sciences,* 79, 424. https://doi.org/10.1007/s12665-020-09159-0

Zhou, D., Xiao, J., Bonafoni, S., Berger, C., Deilani, K., Zhou, Y., Frolking, S., Yao, R., Qiao, Z., & Sobrino, J. A. (2019). Satellite remote sensing of surface urban heat islands: Progress, challenges, and perspectives. *Remote Sensing*, 11(1), 48. https://doi.org/10.3390/rs11010048

8. Appendices

Appendix A: *Supplemental Figures*

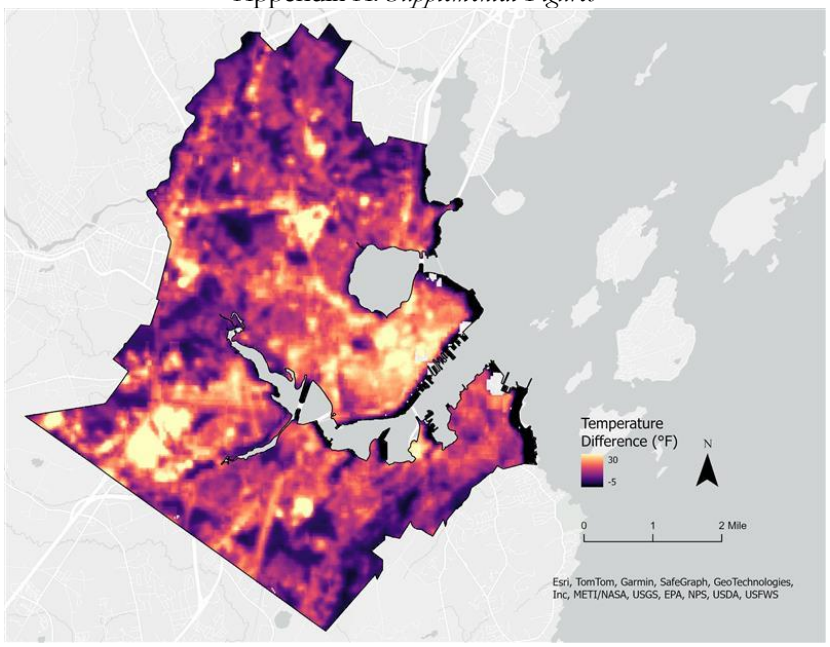

Figure A1: Daytime Urban Heat Assessment Map Pre-Shift

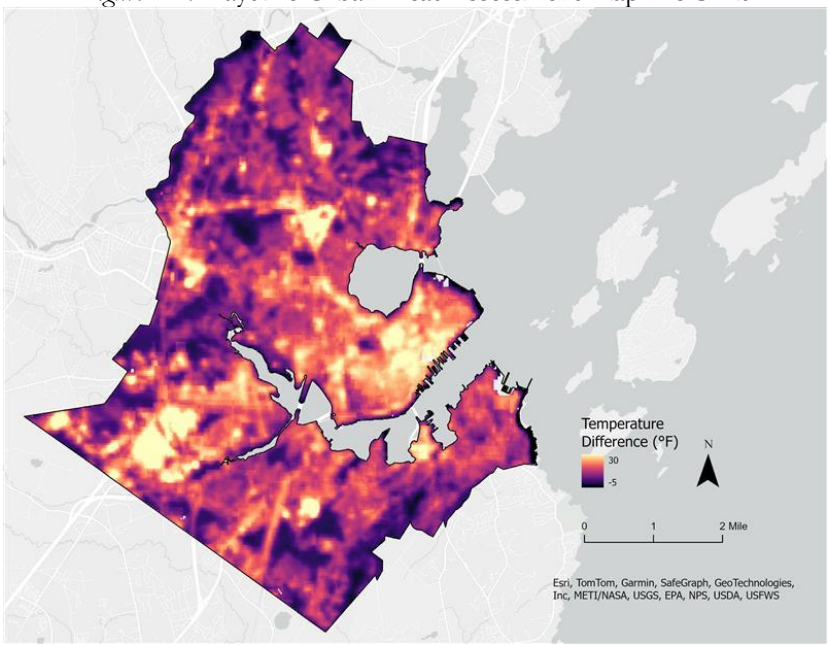

Figure A2: Daytime Urban Heat Assessment Map Post-Shift

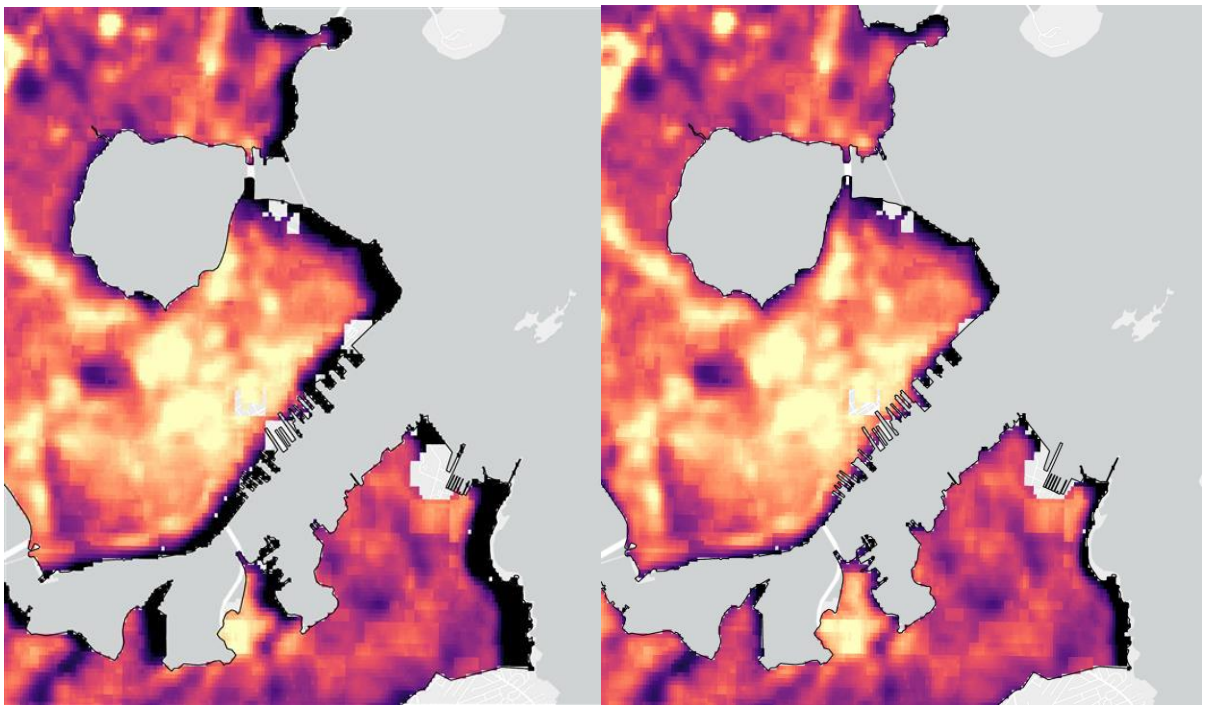

Figure A3: Zoomed in images of Daytime Urban Heat Assessment pre (left) and post (right) shift

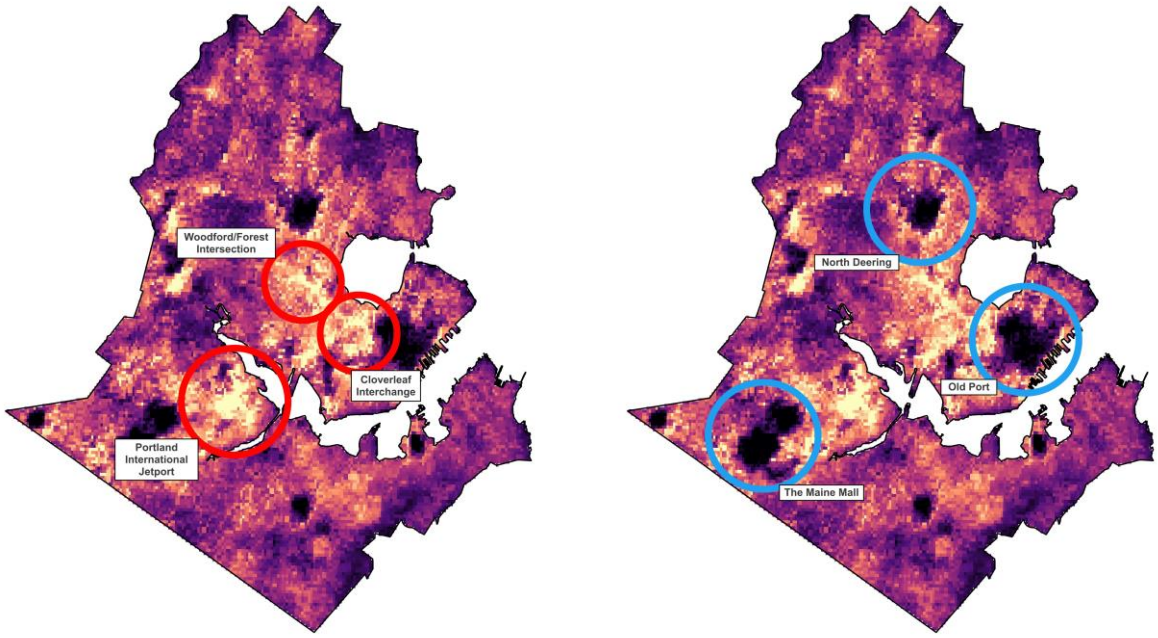

Figure A4: ECOSTRESS Nighttime Urban Heat Assessment Composite Map (2018 – 2024) depicting prominent hot spots (left) and cool spots (right)

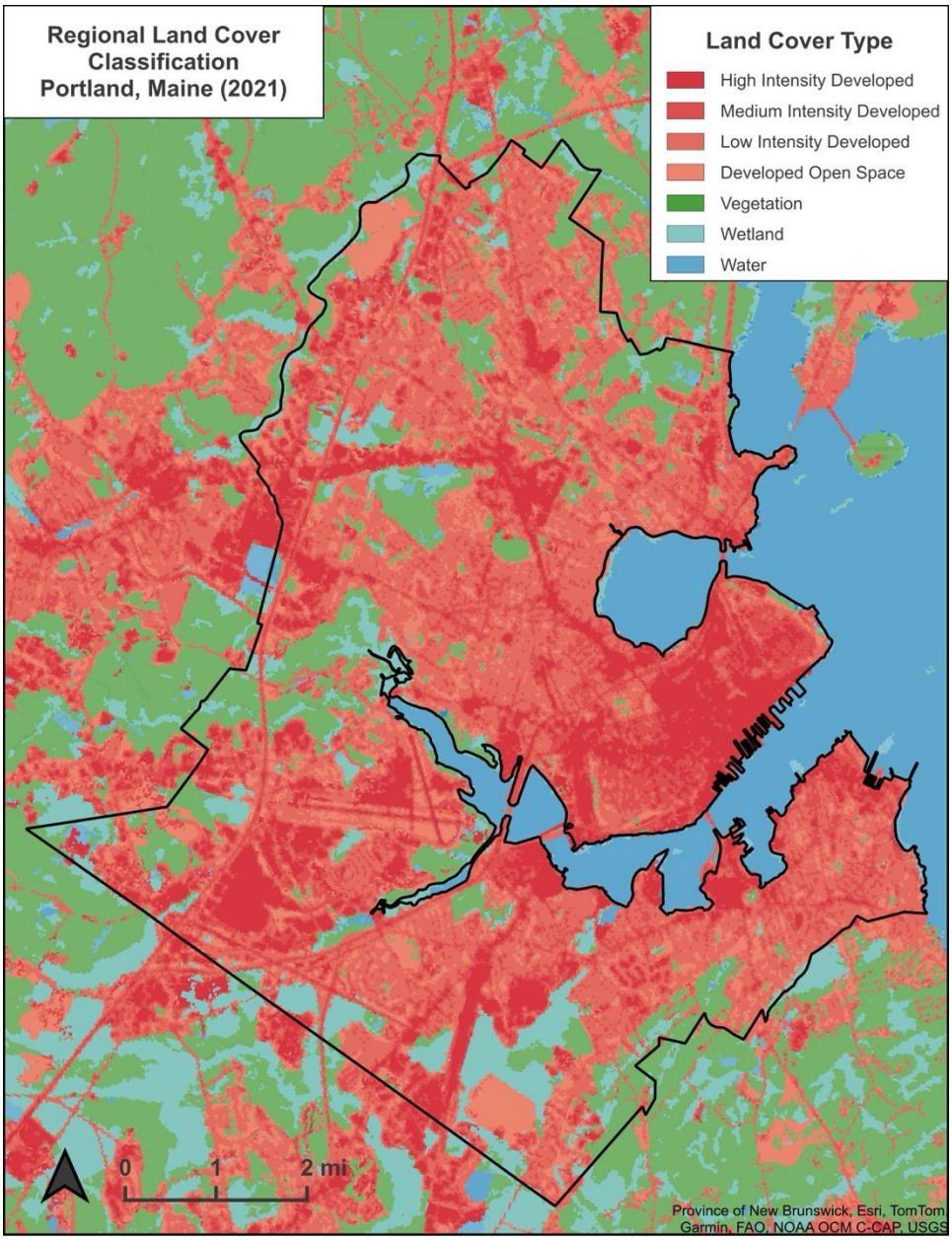

Figure A5: Regional Land Cover Classification for Portland and South Portland, Maine

Figure A6: Mosaiced image of the Urban Heat Mitigation Model output for census tracts 000300, 000500, 000600, 001100, and 001200 on the peninsula of Portland: the five hottest identified from the Urban Heat Vulnerability Map